OE Optical Engineering

RESEARCH PAPER

Ultraviolet and blue stimulated emission from Cs alkali vapor pumped using two-photon absorption and four-wave mixing

Ricardo C. Davila,[a] Christopher A. Rice,[b] Nathan B. Terry,[b,*] and Glen P. Perram[b]

[a]Radiance Technologies, Beavercreek, Ohio, United States

[b]Air Force Institute of Technology, Department of Engineering Physics, Wright-Patterson AFB, Ohio, United States

ABSTRACT. Stimulated emission on the ultraviolet and blue transitions in Cs has been achieved by pumping via two-photon absorption and four-wave mixing for the pump transition $6^2S_{\frac{1}{2}} \rightarrow 8^2D_{\frac{3}{2},\frac{5}{2}}$. The emission performance of the optically pumped cesium vapor laser operating in ultraviolet and blue has been extended to 650 nJ/pulse for 387 nm, 1 to 3 μJ/pulse for 388 nm, 200 nJ/pulse for 455 nm, and 500 nJ/pulse for 459 nm. Emission performance improves dramatically as the cesium vapor density is increased, and no scaling limitations associated with energy pooling or ionization kinetics have been observed.

Keywords: alkali laser; optically pumped alkali vapor laser; four-wave mixing; two-photon absorption

Paper 20240588G received Jul. 2, 2024; revised Nov. 4, 2024; accepted Nov. 7, 2024; published Dec. 9, 2024.

1 Introduction

1.1 Motivation for DPAL Research

Diode-pumped alkali lasers (DPALs) provide high-power and multi-wavelength output, advantages not found in other laser systems that uniquely benefit many applications.[1] The DPAL is pumped by diode bars or stacks through the alkali's D_2 transition to its $^2P_{3/2}$ state, then collisionally relaxed to the $^2P_{1/2}$ state where it lases in the near-infrared (NIR) spectrum along the D_1 transition. DPAL performance is optimized when spin-orbit relaxation with a buffer gas (usually a rare gas or small hydrocarbon) is much faster than the optical excitation rate.[2–4] A rubidium DPAL was first demonstrated in 2003,[5] and in less than 10 years, these laser systems have been scaled to kilowatt power levels,[6,7] analytic lasing models have been developed,[2,3,8] and operating optically pumped alkali vapor laser wavelengths have been verified to span the atmospheric transmission window.[9,10] The alkali gain medium's ability to produce various beams at a variety of wavelengths from ultraviolet through long-wave infrared is a versatility that requires further study and measurement.[11–14] Several comprehensive DPAL reviews[4,15,16] outline the benefits of this laser's high quantum efficiency, gaseous gain medium, reduced thermal issues, diode pumping, and scalability to high output powers. This paper examines two key characteristics of a Cs alkali laser: (a) the interplay of amplified spontaneous emission, two-photon absorption, and four-wave mixing as pumping mechanisms and (b) the relation among temperature, vapor density, and laser output power.

*Address all correspondence to Nathan B. Terry, nathan.terry@afit.edu

1.2 Experimental Context

The interplay of amplified spontaneous emission, two-photon absorption, and four-wave mixing in alkali vapor lasers is explained in several ways. Gai et al.[11] showed that modulating a cesium vapor laser with an infrared laser modulated the UV and blue laser output and concluded that amplified spontaneous emission and four-wave mixing were the key operating mechanisms. Pitz et al.[17] theorized that both cascade lasing and four-wave mixing may both be occurring and may also be in competition with one another for producing the blue beam. Sell et al.[18] examined Rb vapor lasers and arrived at a similar conclusion. In contrast, Sulham et al.[14] concluded that two-photon absorption was the key mechanism for explaining Rb and Cs alkali laser output. Our experiments and analysis provide additional evidence that multiple transition mechanisms are involved.

Along with focusing on the optical transition mechanisms, considerable research examined other mechanisms to improve the performance of alkali lasers,[15] including the uses of buffer gases,[17] the relative advantages of transverse and longitudinal pumping,[15] and the role of heat transfer.[19] Substantial work has also examined the role of temperature and density in Rb and K vapor lasers. For a K vapor cell at 553 K with 5.4 torr of helium (He) buffer gas, Pitz et al.[17] reported that the threshold was ~1 mJ/pulse and the slope efficiency for the blue beam increased by a factor of 4 as the number density increased by a factor of 2.5. Studies of Rb lasers showed that at a cell temperature of $T = 140$°C, 100 mW of ultraviolet light at 398 nm was measured as a harmonic to 1 W of a 794.8-nm beam.[20] In another Rb laser, the maximum output power was 3.2 μJ for a pump power of 3.3 mJ, and slope efficiencies increased from 0.03% to 0.5% for Rb as cell temperatures increased from $T = 175$°C through 250°C. Cs blue emission studies performed in Ref. 14 showed efficiencies on the order of 0.02% to 0.06% for $T = 175$°C to 200°C for pump transition ($6^2S_{1/2} \rightarrow 7^2D_{3/2}$) and blue emissions for the Cs ($7^2P_{3/2,1/2} \rightarrow 6^2S_{1/2}$) transition. For a scaled Cs system, 10 μJ per pulse was achieved for 100 mW, 4-ns pump pulse at 10 Hz.[14] Recent measurements in Ref. 11 reported Cs ultraviolet ($8^2P_{3/2} \rightarrow 6^2S_{1/2}$) and blue ($7^2P_{3/2} \rightarrow 6^2S_{1/2}$) emissions after pumping the $6^2S_{1/2} \rightarrow 7^2D_{5/2}$ transition. Maximum powers achieved in this experiment were 700 and 150 nJ for the ultraviolet and blue emissions, respectively, for a pump pulse power of 0.8 mJ.[11] These findings highlight the role of temperature and density in Rb and K laser operation. In contrast, the role of temperature and vapor density in Cs alkali lasers has received less attention.

1.3 Overview of Experimental Results

This work extends the optically pumped Cs vapor cell transition $6^2S_{\frac{1}{2}} \rightarrow 7^2D_{\frac{5}{2}}$ ultraviolet and blue emissions characterization study outlined in Ref. 11 by including the emissions for the Cs vapor cell pump transition $6^2S_{\frac{1}{2}} \rightarrow 7^2D_{\frac{3}{2}}$. A functional form equation detailed in Ref. 21 to quantitatively evaluate Rb near IR laser energy at 2.73 and 2.79 m for Rb vapor cell transitions $6^2P_{3/2,1/2} \rightarrow 6^2S_{1/2}$, respectively, was applied in this study to assess the Cs ultraviolet and blue emissions. This equation, although not a theoretical solution to the Cs vapor cell emission performance, is sufficient to represent the pump threshold, bleached limit, and slope efficiency dependence on pump energy, providing further validation for the functional fit. Last, this study extends the Cs vapor cell blue emission dependence on Cs vapor density and temperature outlined in Ref. 14 by including visible emissions at 150°C and validating that pump pulse versus blue beam energy dependence detailed in Ref. 14 includes ultraviolet $8^2P_{3/2,1/2} \rightarrow 6^2S_{1/2}$ as well as blue $7^2P_{3/2,1/2} \rightarrow 6^2S_{1/2}$ emissions. The energy levels of Cs are shown in Fig. 1.

2 Experimental Setup

The apparatus for the two-photon ultraviolet and blue emissions study for pump transitions $6^2S_{\frac{1}{2}} \rightarrow 7^2D_{\frac{5}{2},\frac{3}{2}}$ is shown in Fig. 2. A frequency-doubled Quanta-Ray Pro Series pulsed Nd:YAG laser (10 Hz, 0 to 1 J/pulse, 532 nm) was used to pump a Sirah model PRSC-D-1800 dye laser with LDS-765 dye tuned to populate the Cs $7^2D_{\frac{5}{2}}$ or $7^2D_{\frac{3}{2}}$ levels. The dye laser provided 6 to 10 ns pulses in a 1-mm radius spot as the energy was tuned from 0 to 30 mJ per pulse by varying the Nd:YAG flash-lamp energy. A 2.5-cm diameter by 6.5-cm-long Triad technologies cesium

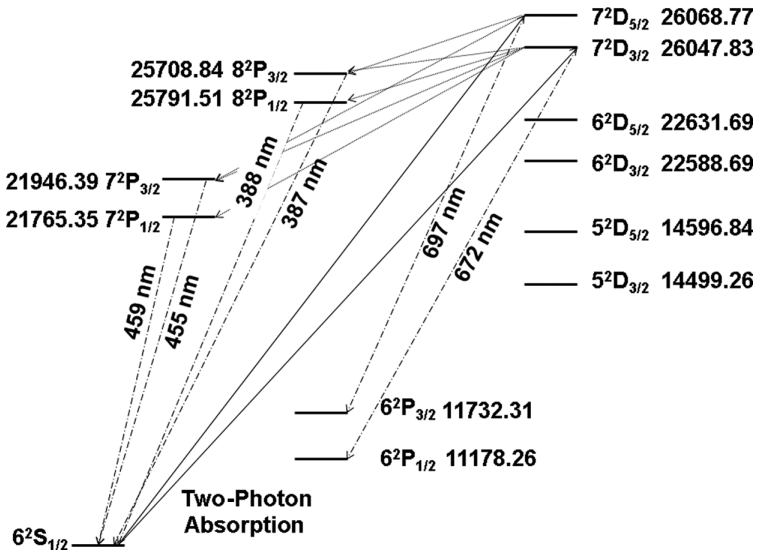

Fig. 1 Cs energy levels.

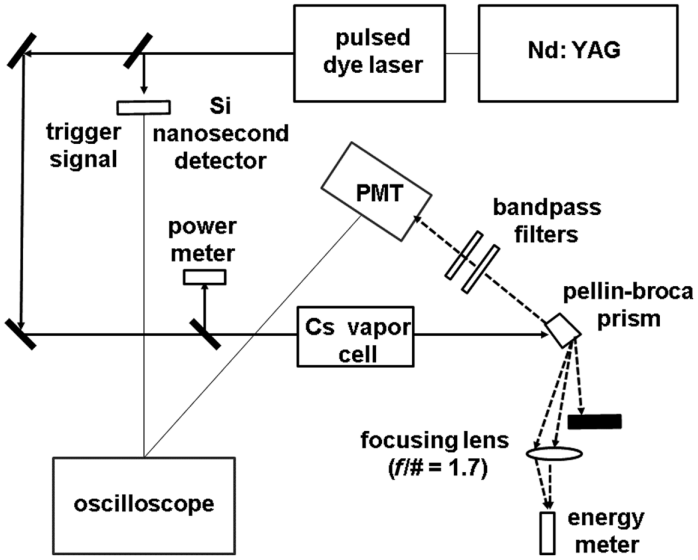

Fig. 2 Cs vapor amplified spontaneous emission (ASE) laser apparatus.

vapor cell with Pyrex windows was heated to 150°C to 200°C. This was a low-pressure cell with no buffer gases and contained only cesium. The target states, Cs $7^2D_{\frac{3}{2}}$ and Cs $7^2D_{\frac{5}{2}}$, are produced by two-photon absorption of the ground state, Cs $6^2S_{1/2}$, at wavelengths near 767.8 and 767.2 nm, respectively. The transmitted pump and resulting stimulated beams were dispersed through a Pellin-Broca prism, reflected off a smooth aluminum block, and measured by the C31034A photomultiplier tube using narrow bandpass filters to isolate the ultraviolet (UV), blue, and red beams. A combination of 25-mm-diameter narrow bandpass filters was used for 387-, 388-, 455-, and 459-nm emission measurements. These filters included a Thorlabs 700-nm short pass filter with a 10% to 15% transition for UV/blue, Edmund optics 452 nm /45 nm bandwidth, a Thorlabs 390 nm /10 nm bandwidth, and specially made bandpass filters from Andover corporation (388.8 nm/1 nm bandwidth, 387.8 nm/1 nm bandwidth, 455.5 nm/3 nm bandwidth, and 459.3 nm/3 nm bandwidth). Average power (emission only) was measured using an RjP-735 pyroelectric energy meter with a spectral response of 0.18 to 20 μm and a minimum detectable energy of 100 nJ.

Blue and UV beams were observed as the pump laser was tuned through the two-photon absorption wavelengths. Visible images of the blue and UV beams and the transmitted far red

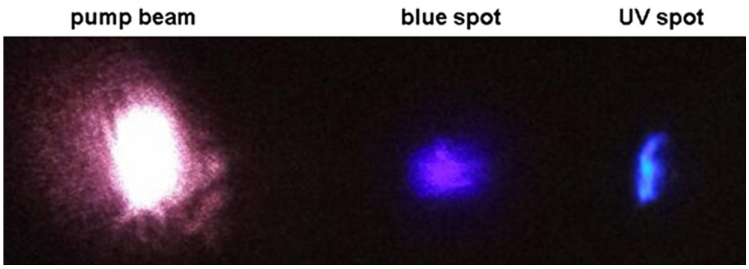

Fig. 3 Beam emissions for the Cs cell in the forward direction at 0.5 m.

pump laser spots recorded after the Pellin–Broca prism for the Cs cell are shown in Fig. 3 at distances of 0.5 and 1.5 m, respectively. Images of the blue and UV beams were taken by a Canon Digital Rebel XT DSLR Camera with EFS 18 to 55 mm f3.5-5.6 zoom lens and 8.0-megapixel CMOS sensor, and video was recorded on a Kodak EasyShare C180 10.2-megapixel digital camera for UV, blue, and red beam emission analysis. The pump beam saturated the camera, whereas the shorter wavelength blue and ultraviolet beams, which diffract less and maintain a more focused profile, were captured via fluorescence from a thin white paper background.

To validate that Cs alkali atoms emit various laser emissions at different wavelengths when pumped on the two-photon Cs $6^2S_{\frac{1}{2}} \rightarrow 7^2D_{\frac{5}{2},\frac{3}{2}}$ transitions, a Cs heatpipe cell was operated at 200°C, corresponding to a Cs vapor density of $n = 1.8 \times 10^{15}$ cm^{-3}, to produce the excitation spectrum shown in Fig. 4. The Cs DPAL cell path was a 12-cm long and 2.54-cm diameter heatpipe pumped by the dye laser using LDS-765 dye at 10 mJ per pulse. The heatpipe, described in detail in Ref. 22, was monitored by a MKS Instruments 690A Baratron capacitance manometer to ensure emission measurements were conducted, whereas the heatpipe contained no or minimal non-Cs vapor gases. The Cs heatpipe cell emissions were collected by SpectraPro-275 and McPherson-218 monochromators to capture emissions from UV (>386 nm) through NIR (<1500) nm with resolutions less than 0:1 nm, sufficient to differentiate between closely space Cs vapor emissions such as 387.6 and 388.9 nm $(8^2P_{\frac{3}{2},\frac{1}{2}} \rightarrow 6^2S_{\frac{1}{2}})$ and 697.3 and 698.3 nm $(7D_{\frac{5}{2},\frac{3}{2}} \rightarrow 6^2P_{\frac{3}{2}})$.

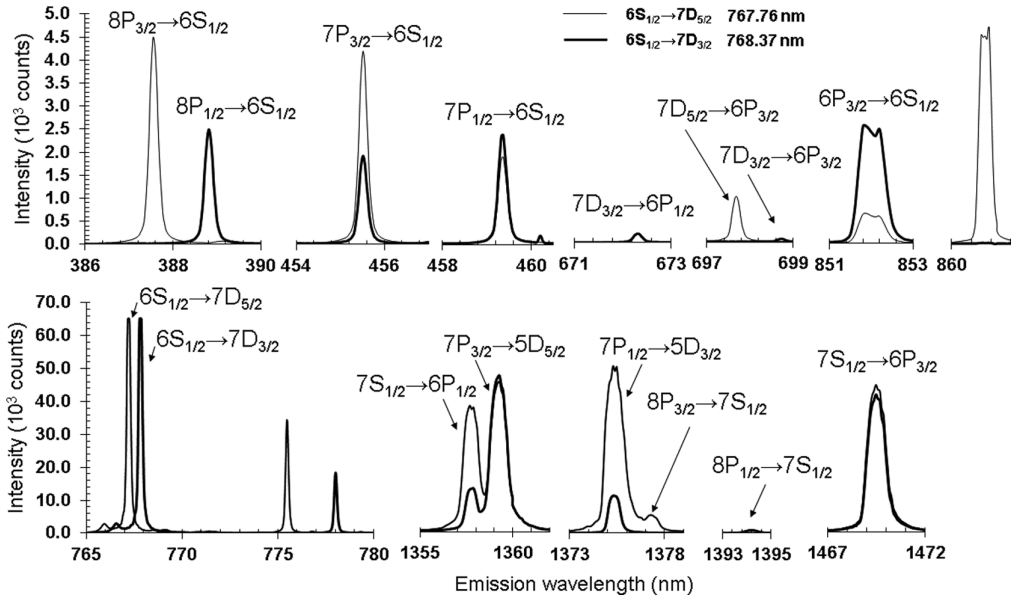

Fig. 4 Cesium emission spectrum for $\lambda = 386$ nm to $\lambda = 1472$ nm for pulsed excitation on the two-photon excitation on the Cs $6^2S_{1/2} \rightarrow 7^2D_{5/2,3/2}$ transitions at heatpipe cell temperature $T = 200$°C.

3 Results

This section evaluates the impact of density and temperature on Cs alkali lasers by describing the laser performance in terms of its emission spectrum, the laser pulse evolution, and the laser power output.

3.1 Cs Emission Spectrum

Figure 4 shows the partial Cs emission spectrum from ultraviolet (>386 nm) through NIR (<1500) nm for pump transitions $6^2P_{\frac{1}{2}} \rightarrow 7^2D_{\frac{5}{2},\frac{3}{2}}$. This figure shows the emission wavelength diversity at a temperature and associated Cs vapor density of 200°C and $n = 1.8 \times 10^{15}$ cm^3, respectively. Our emission results, in several cases, were amplified extensions of the full Cs fluorescence from (>360 nm) through NIR (<1600) nm reported in Ref. 23 with the exception of our recorded emission wavelengths 775.5, 778.0, and 861.7 nm, which have no corresponding fluorescence signatures in Ref. 23. The full spectrum Cs vapor measurements in Ref. 23 were taken at a cell temperature of 247°C (Cs vapor density of $n = 8.9 \times 10^{15}$cm^3) after pump excitation of 455.7 nm $6^2S_{\frac{1}{2}} \rightarrow 7^2P_{\frac{3}{2}}$. The spectrum in Ref. 23 showed atomic transitions up to the ionization limit. The different pumping schemes and Cs cell temperatures between our measurements and the fluorescence spectrum in Ref. 23 may account for the differing emissions in our results.[23] The spectrum in Ref. 23 shows evidence of ionization in the plasma broadening of higher F states and blue Cs recombination continuum between 430 and 510 nm not observed in our measurements as well as weak forbidden transitions $nP_{\frac{3}{2}} \rightarrow 6P_{\frac{3}{2}}$ for $n = 9$, 10, and 11 in Ref. 23 not present in our observations.

3.2 ASE Laser Pulse Evolution

Figure 5 shows 672.3-nm lasing output for Cs vapor cell temperature of 150°C for pump beam energies less than 8 mJ using the equipment setup in Fig. 2. The target state, Cs $7^2D_{3/2}$, was produced by two-photon absorption of the ground state, Cs $6^2S_{\frac{1}{2}}$ at a wavelength near 767.8 nm. The lasing was detected by a C31034A photomultiplier tube with narrow bandpass filters. A Thorlabs FES0750 short-pass filter with a cutoff wavelength of 750 nm was used to minimize scattered pump light yet also allowed over 88% transmission for 672.3-nm emissions. A second Andover Corp 670.8-nm filter with a center wavelength and 10-nm bandwidth filter was used in conjunction with the short-pass filter.

The 670.8-nm filter had a 66% transmission at 672.3 nm. The scattered pump laser intensity was measured and subtracted from the observed emission profiles by tuning off resonance, thereby minimizing the scattered light contribution to the $7^2D_{\frac{3}{2}} \rightarrow 6^2P_{\frac{1}{2}}$ transition emission. Energy measurements could not be performed for 672.3-nm output beams due to the minimal

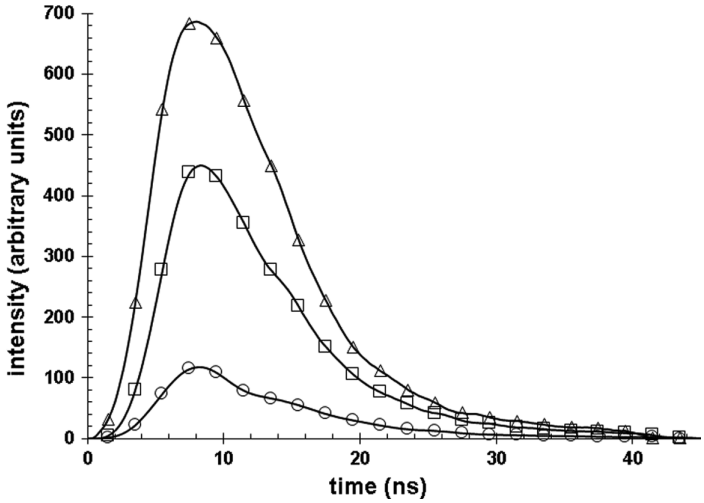

Fig. 5 Cs 672.3 nm ($7^2D_{3/2} \rightarrow 6^2P_{1/2}$ laser output for cell temperature $T = 150$°C and pump energies of ○—5.8 mJ, □—6.9 mJ, and △—7.6 mJ.

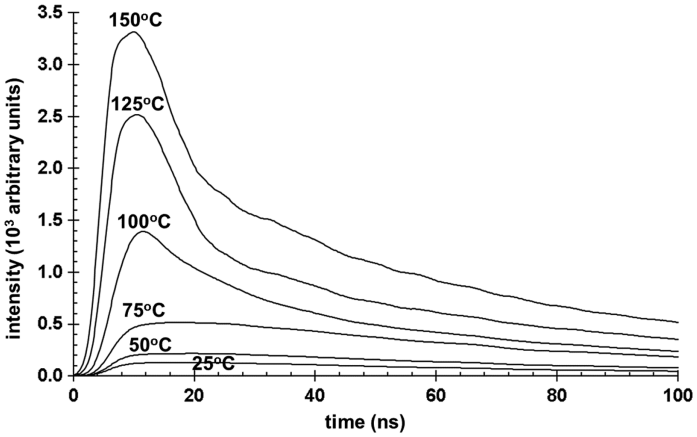

Fig. 6 Cs 672.3 nm ($7^2D_{3/2} \rightarrow 6^2P_{1/2}$) laser development from florescence Cs vapor at $T = 25$°C through laser emissions at $T = 100$°C through $T = 150$°C.

separation between red ASE and pump beam as well as the associated damage risk presented to the RjP-735 pyroelectric energy meter detector. Pump energies were kept below 8 mJ per pulse due to saturation effects on the C31034A photomultiplier for pump pulse energies above this energy per pulse level. ASE at 672.3 nm was also observed for vapor cell temperatures at 175°C and 200°C, and initial indications suggest for a given pump intensity, 672.3-nm ASE intensity increases for higher Cs alkali density. Clearly, 672.3-nm lasing occurred at 150°C, and beam output increased with increasing pump energies. A more detailed analysis is required to determine how the Cs red beam output scales with alkali density and pump intensity and what Cs vapor density is required for the onset of red lasing.

Figure 6 shows the evolution from fluorescence emission (heatpipe temperature < 75°C) for laser beam output (heatpipe temperature > 100°C) for Cs emission 672.3 nm $7^2D_{\frac{3}{2}} \rightarrow 6^2P_{\frac{1}{2}}$. The target state, Cs $7^2D_{\frac{3}{2}}$, was produced by two-photon absorption of the ground state, Cs $6^2S_{\frac{1}{2}}$, at wavelength 767.8 nm. The population of the excited state was measured using the C31034A photomultiplier tube to detect the side fluorescence for temperatures at and below 75°C and lasing emissions for Cs heatpipe temperatures at or above 100°C. Figure 6 indicates that 672.3-nm lasing onset occurred between cell temperatures of $T = 75$°C and $T = 100$°C corresponding to Cs vapor densities of $n = 3.1 \times 10^{12}$ cm^3 and $n = 1.5 \times 10^{13}$ cm^3, respectively. The rapid decrease in intensity at $T = 100$°C after reaching peak intensity compared with longer measured decay rates at $T = 75$°C and below, consistent with previous fluorescence decay profiles,[24,25] is indicative of pulsed lasing activity. The time scale of these emissions for cell temperatures $T = 100$°C approaches pulses of 20 to 30 ns, roughly two to three times the 10 ns pump pulse duration. Figure 6 also confirms previous observations made during the 7D spin-orbit study[24] that heatpipe temperatures above 75°C result in longer decay rates due to radiation being absorbed and remitted before escaping the heat pipe. The laser dye pump pulse at the entrance window of the heatpipe was ~16 mJ per pulse.

3.3 ASE Laser Output

The dependence of the ultraviolet and blue output energies on pump energy at three temperatures for the pump transitions $6^2S_{\frac{1}{2}} \rightarrow 7^2D_{\frac{5}{2}}$ and $6^2S_{\frac{1}{2}} \rightarrow 7^2D_{\frac{3}{2}}$ are shown in Figs. 7 and 8, respectively. Output energies grow linearly until pump pulse energies of 6 to 8 mJ and gradually level off through the highest pump energy used at 31 mJ. For all emission wavelengths, the energies increased with cesium vapor density. The uncertainty in the output energies represents the 95% confidence bounds for the associated lasing intensities measured by the C31034A photomultiplier tube. A functional form, first used and described in Ref. 21, was used to fit these results

$$E = E_m\left(1 - e^{-\eta\left(\frac{(E_p - E_{\text{th}})}{E_m}\right)}\right), \tag{1}$$

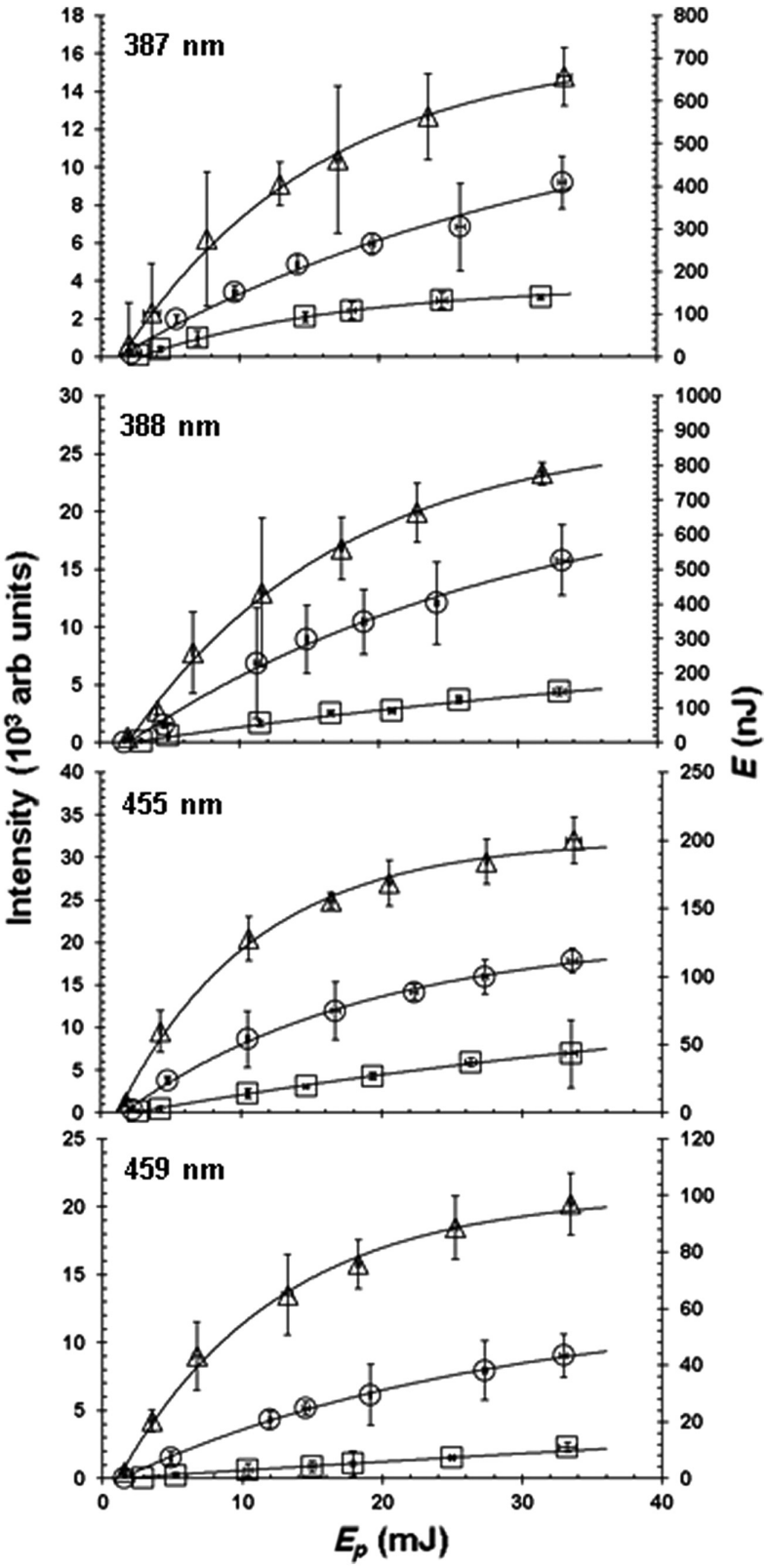

Fig. 7 Ultraviolet (387, 388 nm) and visible (455, 459 nm) for pump transitions $6^2S_{\frac{1}{2}} \rightarrow 7^2D_{5/2}$ for three temperatures and corresponding Cs vapor densities: (□) $T = 150°C$, $n = 2.26 \times 10^{14}$ cm^{-3}, (○) $T = 175°C$, $n = 6.81 \times 10^{14}$ cm^{-3}, and (△) $T = 200°C$, $n = 1.82 \times 10^{15}$ cm^{-3}.

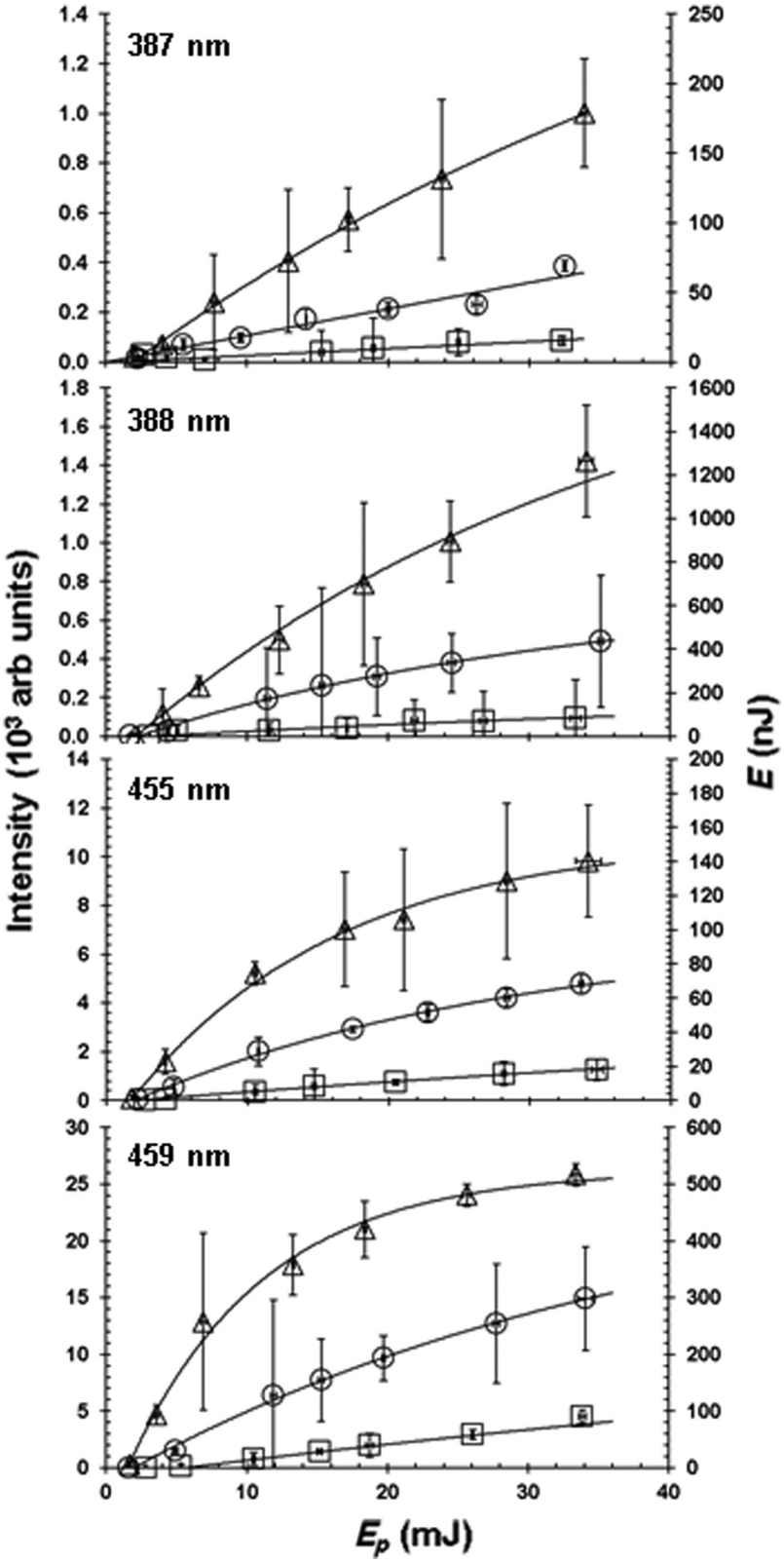

Fig. 8 Ultraviolet (387, 388 nm) and visible (455, 459 nm) for pump transition $6^2S_{1/2} \rightarrow 7^2D_{3/2}$ for three temperatures and corresponding Cs vapor densities: (□) $T = 150°C$, $n = 2.26 \times 10^{14}$ cm^{-3}, (○) $T = 175°C$, $n = 6.81 \times 10^{14}$ cm^{-3}, and (△) $T = 200°C$, $n = 1.82 \times 10^{15}$ cm^{-3}.

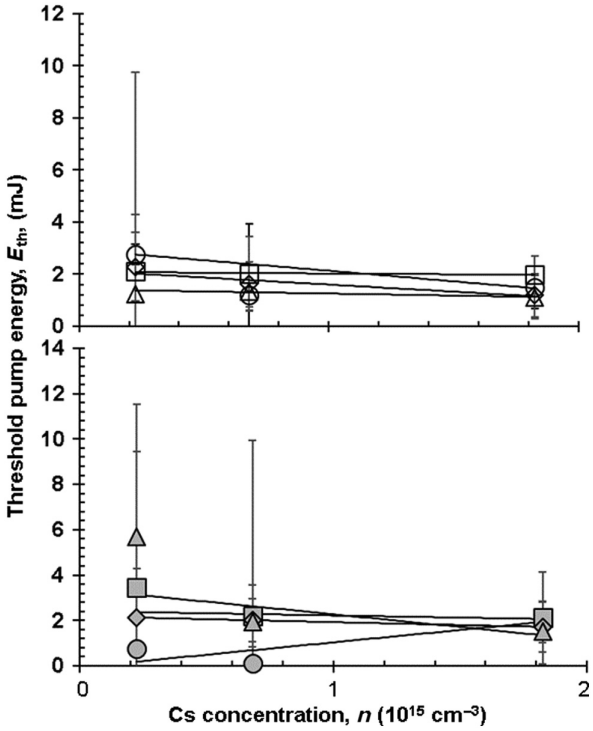

Fig. 9 Dependence of the initial energy, E'th, on the cesium density, when pumping $6^2S_{1/2} \rightarrow 7^2D_{5/2}$ (open symbols) and $6^2S_{1/2} \rightarrow 7^2D_{3/2}$ (filled symbols) for 387 nm (○, •), 388 nm (□, ■), 455 nm (◇, ◆), and 459 nm (△,▲).

where E is the laser output energy per pulse, E_p is the pump dye laser energy per pulse, E_m is the bleached limit for maximum output energy, E_{th} is the threshold pump energy, and η is the initial slope efficiency.

Threshold conditions were achieved for both pump transitions for pump energies of 0.5 to 3.5 mJ, as shown in Fig. 9. Error bounds in Fig. 9 are reported for the 95% confidence intervals for the E_{th} fit parameter. Consistent with results reported in Ref. 21, for higher pump intensities, there were not sufficient cesium atoms in the pumped volume to process all the incident pump photons. The population in the ground state was depleted, and the pump transition became transparent. As the alkali density increased, the maximum output energy increased linearly because additional pump photons can be processed. The linear fits in Fig. 10 indicate a small positive intercept, which could be interpreted as a threshold requirement or may indicate minor curvature at higher alkali densities. For both pump transitions, the trend is for the ultraviolet emissions (387, 388) nm to reach higher bleached limits than the blue (455, 459) nm transitions; however, the results from Eq. (1) were insufficient to adequately capture the E_m for 387 nm emission for pump transition $6^2S_{\frac{1}{2}} \rightarrow 7^2D_{\frac{3}{2}}$. Error bounds in Fig. 10 are reported for the 95% confidence intervals for the E_m fit parameter. The slope efficiencies in Fig. 11 also improve as the Cs density increases. The threshold for the ASE beams for both ultraviolet and blue occurred for Cs densities at $T = 120$°C (Cs density of $n = 4.9 \times 10^{13}$).

4 Discussion

Analyzing the output energy as a function of the input energy of the cesium reveals the saturation intensity and the slope efficiency of the cesium cell, which are key parameters to understanding the scaling potential of cesium-based DPAL lasers. At the same time, these results underscore the potential wavelength tunability of cesium-based DPAL devices. We clarify the wavelength tunability by briefly reconsidering the excitation pathways of cesium-based DPAL lasers.

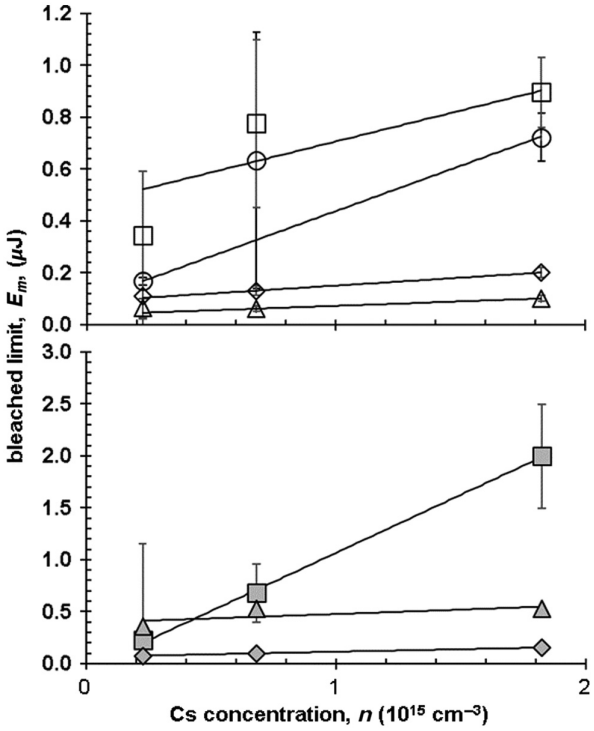

Fig. 10 Dependence of the maximum achieved output energy, *Em*, on cesium density when pumping $6^2S_{1/2} \rightarrow 7^2D_{5/2}$ (open symbols) and $6^2S_{1/2} \rightarrow 7^2D_{3/2}$ (filled symbols) for 387 nm (○, •), 388 nm (□, ■), 455 nm (◇, ◆), and 459 nm (△,▲).

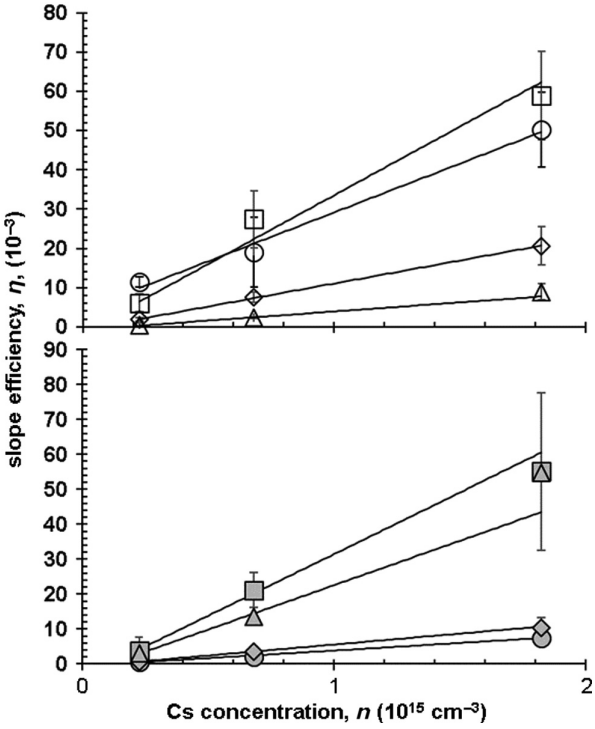

Fig. 11 Dependence of the initial slope efficiency, η, on cesium density when pumping $6^2S_{1/2} \rightarrow 7^2D_{5/2}$ (open symbols) and $6^2S_{1/2} \rightarrow 7^2D_{3/2}$ (filled symbols) for 387 nm (○, •), 388 nm (□, ■), 455 nm (◇, ◆) and 459 (△,▲).

4.1 Two-Photon Saturation Intensity

Both threshold and pump efficiency should depend on the absorption cross-section. Two-photon absorption cross-sections are quite low. Although Cs two-photon cross-sections have not been reported in the literature, calculations using a methodology outlined in Ref. 15 predict two-photon cross-sections for pump transitions $6^2S_{\frac{1}{2}} \rightarrow 7^2D_{\frac{5}{2},\frac{3}{2}}$ to be 6.0×10^{21} cm^4/W and 2.5×10^{21} cm^4/W, respectively. At the threshold pump energy of 3 mJ (the low end of our pump energies), the corresponding pump intensity, I, is 2×10^6 W/cm^2. To derive the two-photon saturation intensity, we consider the time dependence of the excited state number density[26]

$$\frac{dn_e}{dt} = \frac{\sigma_{eg} I_l^2}{h\nu_l} n_g - \Gamma n_e, \tag{2}$$

where n_e is the number density of the excited state, σ_{eg} is the two-photon cross section for the ground state, g, to the excited state, e, I_l is the laser intensity, h is Planck's constant, ν_l is the laser frequency, n_g the number density of the ground state, and Γ is the total decay rate from the upper level in sec^{-1}. For the steady state condition, $dn_e/dt = 0$ and Eq. (2) becomes

$$I_{\text{sat}}^2 = \frac{\Gamma h\nu_l}{\sigma_{eg}}. \tag{3}$$

The saturation intensities, I_{sat} for pump transitions $6^2S_{\frac{1}{2}} \rightarrow 7^2D_{\frac{5}{2},\frac{3}{2}}$, are 30 and 50 kW/cm^2, respectively. With saturation parameters of $S = I/I_{\text{sat}}$ of 64 and 41, the sample is strongly bleached for both pump transitions.

4.2 Optical Excitation Pathways

Although the primary lasing mechanism for many Cesium alkali lasers is often assumed to be two-photon absorption followed by cascade lasing,[14,19,21,24,27] four-wave mixing can also serve as the central transition mechanism. For example, Gai et al.[11] explained the 455.6-nm output from a Cesium vapor cell pumped via 767.2 nm with four-wave mixing, i.e.,

$$2hv_{767.2\text{ nm}} - 1hv_{2.42\ \mu\text{m}} \rightarrow 1hv_{455.6\text{ nm}}.$$

They experimentally demonstrated modulating a 2.42-μm input beam modulated the 455.6-nm output beam, strongly supporting the argument of FWM as the key mechanism. Although Sulham et al.[14] concluded that two-photon absorption was the key mechanism because they observed blue light when the cesium cell was pumped at 743.2, 672.2, and 767.8 nm, they also observed an infrared beam of less than 2.5 μm, which is consistent with the four-wave mixing explanation offered by Gai et al. However, four-wave mixing cannot explain all the laser output we observed because some of the required intermediate transitions, $7^2D_{\frac{5}{2}} \rightarrow 7^2P_{\frac{1}{2}}$ and $7^2D_{\frac{5}{2}} \rightarrow 8^2P_{\frac{1}{2}}$, are forbidden. As photoionization is orders of magnitude less likely than absorption at these wavelengths,[27] we reject photoionization as a plausible mechanism. The excitation pathways are most likely a combination of cascade lasing triggered by two-photon absorption and ASE mediated by FWM.

5 Conclusion

This paper examined the output power of a Cs vapor alkali laser as a function of operating temperature and vapor density. We demonstrated that the UV and blue output scaled linearly with pump pulse energies below 6 to 8 mJ and gradually leveled off at higher pump energies. The slope efficiency increased with cesium density. Finally, this paper examined the lasing mechanisms of a cesium vapor laser and concluded that the UV and blue output beams were produced by a combination of amplified spontaneous emission, four-wave mixing, and two-photon absorption. We also showed how density and temperature impact the performance of Cs vapor alkali lasers.

Code and Data Availability

All data in support of the findings of this paper are available within the article.

Acknowledgments

This paper is based on a PhD Dissertation entitled "Two-Photon Excitation of Cesium Alkali Metal Vapor 7^2D, 8^2D Kinetics and Spectroscopy."

References

1. G. P. Perram et al., *An Introduction to Laser Weapon Systems*, Directed Energy Professional Society (2010).
2. G. D. Hager and G. P. Perram, "A three-level analytic model for alkali metal vapor lasers: part I. Narrowband optical pumping," *Appl. Phys. B: Lasers Opt.* **101**, 45–56 (2010).
3. G. D. Hager and G. P. Perram, "A three-level model for alkali metal vapor lasers. Part II: broadband optical pumping," *Appl. Phys. B: Laser Opt.* **112**, 507–520 (2013).
4. W. F. Krupke, "Diode pumped alkali lasers (DPALs)—a review (rev1)," *Prog. Quantum Electron.* **36**, 4–28 (2012).
5. W. F. Krupke et al., "Resonance transition 795-nm rubidium laser," *Opt. Lett.* **28**, 2336–2338 (2003).
6. A. V. Bogachev et al., "Diode-pumped cesium vapor laser with closed-cycle active medium circulation," *Quantum Electron.* **42**, 95 (2012).
7. G. A. Pitz et al., "Advancements in flowing dioded pumped alkali lasers," *Proc. SPIE* **9729**, 972902 (2016).
8. N. D. Zameroski et al., "Experimental and numerical modeling studies of a pulses rubidium optically pumped alkali metal vapor laser," *J. Opt. Soc. Am. B: Opt. Phys.* **28**, 1088–1099 (2011).
9. G. A. Pitz et al., "Atmospheric propagation properties of various laser system," *Proc. SPIE* **8380**, 83800V (2021).
10. G. P. Perram and C. A. Rice, "Atmospheric transmission for cesium DPAL using TDLAS," *Proc. SPIE* **8238**, 823801 (2012).
11. B. Gai et al., "Modulation of a double-line frequency up-conversion process in cesium vapor," *Appl. Phys. B: Lasers Opt.* **122**, 165 (2016).
12. G. A. Pitz, C. D. Fox, and G. P. Perram, "Pressure broadening and shift of the cesium D2 transition by the noble gases and N_2, H_2, HD, D_2, CH_4, C_2H_6, CF_4, and ^3He with comparison to the D_1 transition," *Phys. Rev. A* **82**(4), 042502 (2010).
13. A. Sharma et al., "Continuous-wave mirrorless lasing in optically pumped atomic Cs and Rb vapors," *Appl. Phys. Lett.* **39**(3), 209–211 (1981).
14. C. V. Sulham, G. A. Pitz, and G. P. Perram, "Blue and infrared stimulated emission from alkali vapors pumped through two-photon absorption," *Appl. Phys. B: Lasers Opt.* **101**(1–2), 57–63 (2010).
15. F. Gao et al., "Review on diode-pumped alkali vapor laser," *Optik* **124**(20), 4353–4358 (2013).
16. B. V. Zhdanov and R. J. Knize, "Review of alkali laser research and development," *Opt. Eng.* **52**(2), 21010 (2013).
17. G. A. Pitz et al., "Two red photon absorption in alkalis producing infrared and blue beams," in *AIAA Plasmadyn. and Lasers Conf. 41st*, Vol. **4876** (2010).
18. J. F. Sell, M. A. Gearba, and R. J. Knize, "Collimated blue and infrared beams generated by two-photon excitation in Rb vapor," *Opt. Lett.* **39**(3), 528 (2014).
19. A. Guofei et al., "Optimizatoin of physical conditions for a diode-pumped cesium vapor laser," *Opt. Express* **25**(4), 4335–4347 (2017).
20. R. J. Lane and A. B. Petersen, "A diode-pumped Rb laser at 398 nm," *Proc. SPIE* **6871**, 68711Q (2008).
21. P. J. Moran et al., "Near infrared rubidium 62P3/2,1/2 and 62S1/2 laser," *Opt. Commun.* **374**, 51–57 (2016).
22. W. Klennert, A. J. Sandavol, and D. A. Hostutler, "Development of a compact heat pipe oven for optically pumped alkali laser research," *J. Directed Energy* **4**, 245–252 (2012).
23. J. Huennekens, Z. Wu, and T. G. Walker, "Ionization, excitation of high lyingatomic states, and molecular fluorescence in Cs vapor excited at =455.7 and 549.4 nm," *Phys. Rev. A* **31**(1), 196–209 (1985).
24. R. C. Davila and G. P. Perram, "Spin-orbit relaxation of cesium 7 2D in mixtures of helium and argon," *Phys. Rev. A: At. Mol. Opt. Phys.* **93**(3), 033418 (2016).
25. R. C. Davila, G. P. Perram, and B. Eschel, "Time-resolved fine structure mixing of cesium 82D induced by helium and argon," *J. Phys. B: At. Mol. Opt. Physi.* **50**(22), 225204 (2017).
26. W. K. Bishel and W. K. Crosley, "Detection of fluorescence from O and N atoms induced by two-photon absorption," *Appl. Opt.* **21**(8), 1419–1429 (1982).
27. B. Oliker, *Examination of Ionization in Cesium Diode Pumped Alkali Lasers with an Ion Chamber Diagnostic*, University of New Mexico (2022).

Ricardo C. Davila is a Spectral Imagery Scientist at Radiance Technologies. He received his BS degree in physics from Concordia College in 1982, his MS degree in space physics from Utah State University in 1992, and his PhD in applied physics from the Air Force Institute of Technology in 2018. His research interests include data science, remote sensing, and atmospheric physics.

Christopher A. Rice is an adjunct professor at the Air Force Institute of Technology. He earned his BS degree from Cedarville University in Electrical Engineering, his MS degree in electrical engineering from AFIT, and his PhD in optical sciences and engineering from AFIT. His research interests include atmospheric laser propagation; diode-pumped alkali and rare gas lasers; aerosol field measurements; modeling, simulation, and validation of directed energy simulations; pulsed laser ablation of titanium and carbon; and turbulence characterization.

Nathan B. Terry is a senior military professor and Interim Department Head of the Engineering Physics Department at the Air Force Institute of Technology. He received his BS and MS degrees in Physics from Brigham Young University in 2000 and 2001, respectively, and his PhD from the Air Force Institute of Technology in 2007. His research interests include fiber lasers and amplifiers, semiconductor lasers, physics education, and nuclear deterrence.

Glen P. Perram is an emeritus professor at the Air Force Institute of Technology. He received his BS degree from Cornell University in 1980, his MS degree from the Air Force Institute of Technology in 1981, and his PhD in physics from the Air Force Institute of Technology in 1986. His research interests include gas lasers, material interactions, remote sensing, spectroscopy, chemical kinetics, optical instruments, diagnostic techniques, and combustion events. He is a fellow of Optica.